Research Article

Ting Su, Wenwen Gao*, Xiangdong Xing, Xinzhe Lan, and Yonghui Song

Optimization for simultaneous removal of NH_3-N and COD from coking wastewater via a three-dimensional electrode system with coal-based electrode materials by RSM method

https://doi.org/10.1515/gps-2021-0072
received July 06, 2021; accepted October 24, 2021

Abstract: The present work demonstrated preparation of coal-based electrode materials (CEM)-derived low-rank coal for simultaneous removal of ammonia nitrogen (NH_3-N) and chemical oxygen demand (COD) from coking wastewater by a three-dimensional electrode system (3DES). The influence of important parameters in 3DES such as processing time, applied voltage, electrode plate spacing, mass of commercially activated carbon (CAC), and initial pH were investigated. Based on the central composite design, the response surface method (RSM) was employed in order to optimize the variable parameters in removal process of pollutants. From the analysis of RSM, the optimum conditions for 3DES were 4.5 h of processing time, 5.5 V of applied voltage, 17 mm electrode plate spacing, 4.5 g CAC, and pH of 3 with higher simultaneous removal rate of COD (74.20%) and NH_3-N (51.48%). Besides, the content of N element (4.9%) and N containing groups were traced by SEM-EDS and FTIR analysis in order to verify the removal effect. The experiment results showed the capability of CEM for electrode system removal of pollutants from coking wastewater and obtained considerable simultaneous removal rate of NH_3-N and COD.

Keywords: NH_3-N and COD, simultaneous removal rate, three-dimensional electrode system, coal-based electrode materials, response surface method

1 Introduction

Coke industry plays an important role in economic construction and social development in China, and it is also one of the pillar industries to maintain the steady economic growth. In 2019, the total production of coke in China was about 471.26 million tons, following which millions of tons of coking wastewater (CW) were produced from coal coking and its by-products refinement [1]. CW is an extremely typical refractory wastewater with high concentration of toxic components and complicated composition owing to the presence of various refractory compounds [2–4]. For decades, one of the most popular methods in CW treatment is the biological treatment, especially the anaerobic–anoxicoxic (A^2/O and A^2/O^2) are the preeminent selection to deal with CW at present [5–9]. Certain results in a large number of research and practice were obtained after the new scientific and effective studies in CW treatment technology; however, the disadvantages of current treatment still exists in two aspects: (i) the content of NH_3-N and COD in the wastewater is still high after advanced treatment and the biochemical properties are poor [9] and (ii) in-depth treatment processes generally have limitations in popularization and application such as high investment costs, high operating costs, harsh reaction conditions, and unstable operation. These problems have attracted more attention to the field of CW treatment technology, which restricted the green and efficient development of coke industry, and thus, more effective approaches for removing NH_3-N and COD in CW need to be explored.

Electro-adsorption and electrochemical technology exhibit great potential in industrial wastewater treatment

* **Corresponding author: Wenwen Gao,** School of Chemistry and Chemical Engineering, Yulin University, Shaanxi Key Laboratory of Low Metamorphic Coal Clean Utilization, Yulin, 719000, China, e-mail: 154167822@qq.com
Ting Su: School of Chemistry and Chemical Engineering, Yulin University, Shaanxi Key Laboratory of Low Metamorphic Coal Clean Utilization, Yulin, 719000, China
Xiangdong Xing, Xinzhe Lan, Yonghui Song: School of Metallurgical Engineering, Xi'an University of Architecture and Technology, Key Laboratory of Gold and Resources of Shaanxi Province, Xi'an, 710055, China

due to its features of wide adaptability, simple equipment, and easy operation [10]. The 3DES has recently drawn considerable attention as an upgraded electrochemical technology because of lower energy consumption in process compared to traditional electrochemical technology [11–13]. The main difference is that there are particle electrodes scattered between the cathode and anode. The particle electrode will be polarized by the applied voltage to form microelectrodes, further, to improve the treatment efficiency as well as reduce the energy consumption [14]. 3DES has been utilized in treatment of dyeing wastewater [14], cyanide wastewater [15], or cyanide tailings [16] to remove toxic and recalcitrant organic contaminants. Therefore, 3DES is suitable to adsorb or decompose the NH_3-N and COD in CW.

Electro-adsorption is not particularly new and has been used for many years in the field of wastewater treatment. While the effluent of the system was generally difficult to meet the biodegradation and nitrification standard of NH_3-N and COD, advanced electrochemical oxidation constitutes a relatively new area which has emerged from 3DES for degradation of the refractory pollutants, better performance on the removal efficiency, and treatment of each kind of pollutant. The previous studies were mainly focused on improving the removal rate of single COD or other pollutant from CW [17–19], and only very few studies are available on the simultaneous removal of NH_3-N and COD by the method of 3DES [20]. In view of the sustainable development of coke industry, the simultaneous removal of these two main pollutants from CW can promote to solve the deep purification treatment problem which has great practical significance.

Hence, a novel 3DES was first constructed in CW treatment. Combining of the electro-adsorption and electrochemical reaction aims to improve the simultaneous removal rate of NH_3-N and COD due to its convenience and economy. The objectives of this work are: (i) to test the properties of CEMs prepared by lab; (ii) to investigate the effect of processing time, applied voltage, electrode plate spacing, mass of commercially activated carbon (CAC), and initial pH on the process performance, and try to disclose the possible mechanism of removal effect of NH_3-N and COD; (iii) to optimize the process conditions with the aim of achieving the maximum of simultaneous removal rate of NH_3-N and COD, while verifying the experimental data and predicted data; and (iv) to characterize the CEMs after process in order to confirm the removal effect of 3DES.

2 Experimental raw materials and characterization methods

2.1 Methods and technological process

First, pre-grading and pyrolysis preprocessing were conducted on the coal sample for further experiment. Next formation and preparation of CEMs were performed for electrosorption with NH_3-N and COD in CW as shown in Figure 1.

The de-ashed coal direct liquefaction residue (DCLR) powder (particle size < 0.15 mm) were used as forming binder in the present experiment, 2.0 g coal powder from SJC (Sunjiacha Coal Mine) after pyrolysis process (P-SJC powder) and DCLR powder were evenly mixed in a stirrer at a rotation speed of 500 rpm for 30 min at a specific mass ratio after drying (mass percentage of P-SJC and DCLR was 5:1), and 0.5 g KOH powder were added to form a tablet sample with the size of $\Phi 30 \times 2$ mm under a pressure of 8.0 MPa by FYD-40-A powder press machine. After drying, the samples underwent pyrolysis process (the final temperature was set as 800°C and the heating rate was 5°C·min^{-1}) and were then treated with nitric acid with a concentration of 40 wt% (wt% of coal-based materials and HNO_3 was 1:3) for 8.0 h. Finally, the samples were washed to neutrality and dried. 3DES was composed of cathode, anode, and particle electrode. Herein the CEMs were used as the anode and cathode, and the CAC was used as the particle electrode. Three pieces of CEMs are connected to the cathode and anode of the DC stabilized power supply. A quantitative amount of CAC was added to electrochemical system and stirred them in the whole process with a magnetic stirrer. 50.0 mL of diluted CW were consumed for batch experiments, and the removal rates of NH_3-N and COD were measured at different conditions.

2.2 Raw materials and CW characteristics in the present experiment

Coal samples were collected from SJC and DCLR were collected from Shenhua Coal Group. Table 1 lists the proximate analysis and ultimate analysis results of SJC, P-SJC, and DCLR. Overall, the contents of carbon were higher with 34.30% volatile, the ash content and sulfur content were lower with 5.94% and 0.42%, respectively, which is a typical kind of high-quality low-rank coal. The

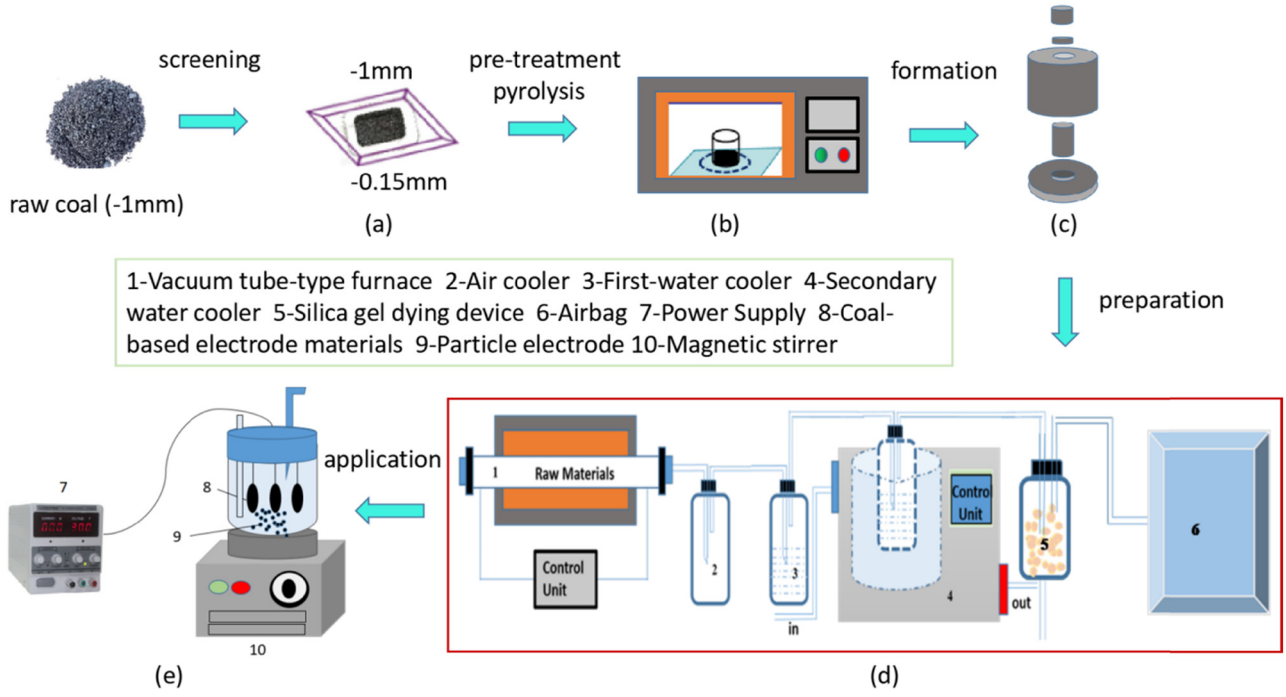

Figure 1: Illustration of experimental process. (a) screening (b) pre-pyrolysis (c) forming process (d) activated process (e) electrochemical system.

CW was taken from the Sanjiang Coal Group in Shaaxi, China. The collected samples were tested as quickly as possible. As shown in Table 2, NH_3-N and COD concentrations are 5,916.4 and 45,000.0 mg·L^{-1}, respectively. And it needs to be diluted 100 times before 3DES treatment.

2.3 Calculation and characterization

The potassium dichromate oxidation method was used to determine the COD concentration with spectrophotometer (Hach, DR2800, USA). NH_3-N was measured by natrium reagent method according to the Chinese national standard (HJ 535-2009). Test reagents of NH_3-N (LH-N2N3-100) and COD (LH-DE-100) were both provided by Lian-Hua Tech Co., Ltd. The removal rate of COD (R_C) and NH_3-N (R_N) were calculated from the equations. A1 and A2 (in Appendix). Scanning electron microscope (SEM, Carl Zeiss, Sigma 300, Germany) was adopted to record and visualize the morphology of the samples. Pore structure and structural changes were observed on the CEMs. The surface functional groups were characterized by Fourier-transform infrared spectrometer (FTIR, Bruker, VERTEX70, Germany). The spectra were recorded from 4,000 to 400 cm^{-1} using a KBr window.

2.4 Treatment of wastewater

2.4.1 Effect of processing time

The electro-adsorption means the contact opportunity of each component interrelates with CEMs, all transfer phenomena such as adsorption is inseparable from contact

Table 1: Proximate and ultimate analysis of SJC and DCLR (%)

Samples	Proximate analysis and ultimate analysis								
	M_t	A_{ad}	V_{ad}	*FC_{ad}	C_{ad}	*O_{ad}	H_{ad}	N_{ad}	$S_{t,ad}$
SJC	4.71	5.94	34.30	55.05	73.07	4.94	4.34	0.96	0.42
P-SJC	2.15	16.77	12.07	69.01	72.88	0.30	1.06	0.88	0.60
DCLR	1.15	10.42	32.24	56.19	78.59	3.26	4.22	0.99	1.26

ad: air-dry basis; M_t: total moisture; A_{ad}: ash content; V_{ad}: volatiles; FC_{ad}: fixed carbon; C_{ad}: carbon; O_{ad}: oxygen; H_{ad}: hydrogen; N_{ad}: nitrogen; $S_{t,ad}$: total sulfur. * by difference.

Table 2: Characteristics of the CW

Parameters	Values	Parameters	Values
COD ($mg \cdot L^{-1}$)	45000.0	SS ($mg \cdot L^{-1}$)	700
pH (–)	8.2	Cyanide ($mg \cdot L^{-1}$)	2.6
NH_3-N ($mg \cdot L^{-1}$)	5916.4		

process, therefore the processing time is a fundamental parameter [18,21–23]. Experiment was executed by mixing 2.0 g CAC with 50.0 mL of target dilution CW in a 150.0 mL beaker before setting up the 3EDS. Fixed the applied voltage at 4.0 V and kept the electrode spacing to 15.0 mm. The pH value of dilution CW was maintained at 8.0. After 150 rpm agitation for a certain time (0.5, 1.0, 2.0, 3.0, 4.0, and 5.0 h), 20 mL of the dilution water after treatment was taken and analyzed for NH_3-N and COD concentration. The results are shown in Figure 2a. Clearly, the R_N and R_C increased quickly from the value of 3.2% and 7.5% in the initial stages of the contact period until 4.0 h to the value of 22.4% and 37.3%, respectively, and then showed a slight downward trend with prolonged contact time of 5.0 h. The increase in removal rate during the initial stages before 4.0 h was contributed to adsorption, electro-adsorption, or electrical chemistry process, because all the active sites on the CEMs were vacant during the first stage. However, after a period of time at 5.0 h, few active sites were available, which lead to the observation of small increase in the uptake of removal rate curve, and the system is in equilibrium. Hence, the suitable time for 3DES treatment process was 4.0 h, and this option will be carried out for further experiments.

2.4.2 Effect of applied voltage

Applied voltage, one of the key parameters in the electrochemical process and the driving force of the whole 3EDS, was further investigated to achieve a cost-effective removal rate. The experimental conditions are mass of CAC was 2.0 g, dilution CW was 50.0 mL, processing time was 4.0 h, pH value was 8.0, electrode spacing was 15.0 mm, and the applied voltages were 0.0, 1.0, 2.0, 3.0, 4.0, 5.0, and 6.0 V. The results are shown in Figure 2b, from which the information can be obtained that a better COD removal performance could be achieved with increasing applied voltage. For instance, when the applied voltage rises from 0.0 to 5.0 V, the R_C had an obvious upward trend and reached to the maximum value of 49.34%, and the R_C was maintained close to this value as the applied voltage continued to increase. R_N also had the same performance. NH_3-N and COD were mainly removed by the several different possible processes or combined action of adsorption, electro-adsorption, and anodic oxidation. No voltage was applied in the adsorption process, whereas applied voltage was conducted at different values in other processes. Only 2.1% and 1.9% removal rate of NH_3-N and COD were obtained, respectively, by adsorption, indicating that the adsorption ability of the cathodes was weak. After a certain applied voltage, there were electric double layers in the 3EDS on the surface of the electrodes and the solution which created electro-adsorption conditions, and the electro-adsorption acted as the primary effect at a lower applied voltage stage. On increasing the applied voltage gradually from 2.0 to 5.0 V, the value of R_C and R_N progressively increased from 24.7% to 49.3% and 16.8% to 55.5%, respectively. This positive tendency could be attributed to two aspects: on the one hand, the driving force shared the consistency with applied voltage, leading to a large number of pollutants quickly migrating via the electric double layer and were finally adsorbed in the electrode plate. On the other hand, the oxygen would be produced by the electrolysis of the anode via Eqs. 1–4, the electrode reactions were improved at higher applied voltage, generating some amounts of $^{\cdot}OH$ (Eq. 4), resulting in the oxidation of NH_3-N and COD. Thus, the R_N and R_C were improved by the combined action of electro-adsorption and oxidation at a higher applied voltage of 5 V which was the optimal operating parameter for further experiments.

$$2H_2O \rightarrow 2H_2 + O_2 \quad (1)$$

$$4OH^- - 4e^- = O_2 + 2H_2O \quad (2)$$

$$4H^+ + 4e^- = 2H_2 \quad (3)$$

$$OH^- - e^- \rightarrow {}^{\cdot}OH \quad (4)$$

2.4.3 Effect of electrode plate spacing

The electrode plate spacing is also an important factor of electrical system because it will affect the mode of the electric double layers. The experiment was carried out under the following conditions: mass of CAC was 2.0 g, dilution CW was 50 mL, processing time was 4.0 h, pH value was 8.0, applied voltage was 5.0 V, and the options of electrode spacing was 5.0, 10.0, 15.0, and 20.0 mm. The results are shown in Figure 2c. Clearly, R_C and R_N increased first and then decreased as the electrode plate spacing got farther. The maximum value of R_C was 55.6% at the electrode plate spacing of 15.0 mm, meanwhile, R_N was also relatively high at 50.8%. Therefore, 15.0 mm was a more optimized option in this experiment. Too large or small electrode plate spacing will affect the function of the electric field, and further affect the driving force of the

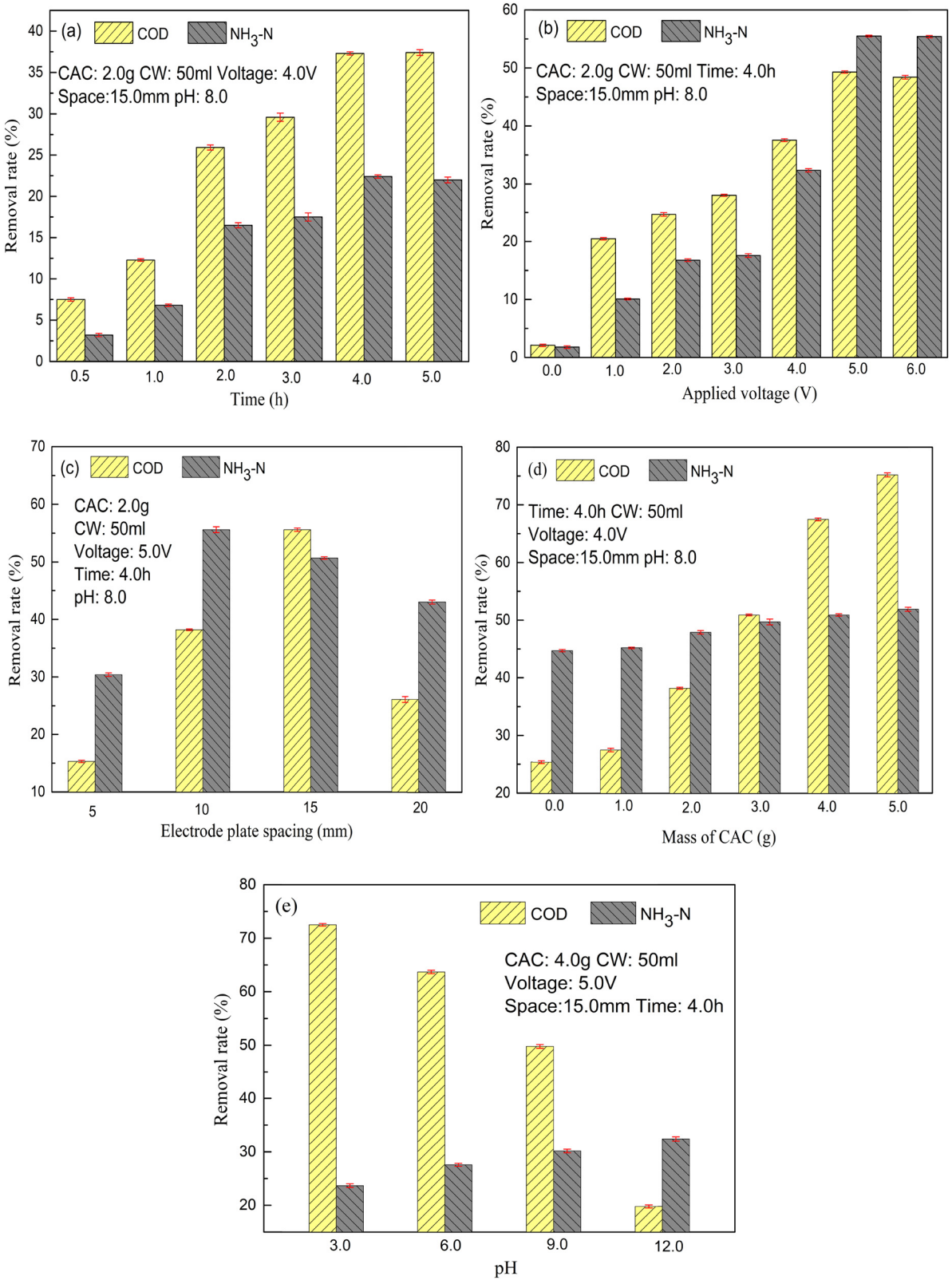

Figure 2: Experiment results of NH_3-N and COD removal rate: (a) processing time, (b) applied voltage, (c) electrode plate spacing, (d) mass of CAC, and (e) initial pH of CW.

electro-chemical reaction. Furthermore, the electrode plate spacing will also affect the effect of the particle electrode. With a suitable distance between the anode and cathode, the electro-chemical reaction rate will be accelerated and achieve a good removal effect finally.

2.4.4 Mass of CAC

As the role of the particle electrode had a great effect in this electrical system because of either the adsorption or electro-chemical effect [24], it was necessary to study the mass of CAC in this experiment. Took 50 mL of dilution CW, set the processing time to 4.0 h, kept the pH value of 8, supplied the applied voltage of 5.0 V, adjusted the electrode spacing to 15.0 mm, and investigated the removal rate when the CAC mass was 0.0, 1.0, 2.0, 3.0, 4.0, and 5.0 g, and the results are shown in Figure 2d. It can be seen that R_C and R_N were 25.4% and 44.7%, respectively, without the CAC addition, which means the two-dimensional electrode system can also obtain a considerable removal effect. Larger mass of CAC was conducive to the improvement of R_C and R_N. The mass of CAC had an obvious impact on R_C, while there was a relatively small impact on R_N because the curve maintained a steady slightly upward trend. The R_C and R_N could reach to 67.56% and 50.9%, respectively, when the CAC mass was 4 g, and the removal rate did not increase significantly when the mass continued to increase. From an economic perspective, the mass of CAC was determined as 4.0 g.

2.4.5 Effect of initial pH

The pH of the CW is about 8.2, and the optimum pH of the electrode system for the COD removal is reported to be 3.0 [25]. It is necessary to analyze the effect of initial pH of dilution CW as a single factor for 3DES treatment [26]. Thus, the degradation performance at different initial pH values (3.0, 6.0, 9.0, and 12.0) was investigated. Meanwhile, the pH value was adjusted by adding a few drops of HCl (1 mol·L^{-1}) and NaOH (1 mol·L^{-1}). Other parameters in the process were kept constant, that is, the mass of CAC was 4.0 g, the processing time was 4.0 h, the applied voltage was 5.0 V, the electrode spacing was 15 mm, and the dilution water volume was 50 mL. It was clearly observed from Figure 2e that R_C was more sensitive to pH than R_N and better COD removal performance could be achieved at lower pH, while a better NH_3-N removal performance could be achieved at higher pH. For instance, the R_C was 72.5% at pH 3.0 whereas it was 19.8% at pH 12, and the R_N was 23.7% at pH 3.0, however it was 32.4% at pH 12.0. More ·OH will be generated under acidic conditions according to literature [27], resulting in higher COD removal efficiency at the lower pH combined with other actions. In contrast, the R_N increased as the initial pH increased from 3.0 to 12.0, this phenomenon could be explained by the form of NH_3-N in the aqueous solution. There are two forms of NH_3-N, as un-ionized ammonia (NH_3) and ionized ammonia (NH_4^+) in the solution, and they can establish an equilibrium via Eq. 5. NH_4^+ was the dominant at low pH, whereas NH_3 was the dominant at high pH. NH_3-N was more likely to be converted to NO_3^- and NO_2^- as per Eqs. 6 and 7 and then converted to N_2 as per Eqs. 8 and 9, but the reactions of Eqs. 6 and 7 occur less often under acidic conditions which could explain the better removal performance of NH_3-N at higher pH state [27]. In order to give attention to two effects of R_N and R_C, pH of 3 was the optimal operating parameter. The process of degradation is shown in Figure 3 [27].

$$NH_3 + H_2O \Leftrightarrow NH_4^+ + OH^- \quad (5)$$

$$NH_3 + 2OH \rightarrow NH_2OH + H_2O \quad (6)$$

$$2NH_2OH + 3H_2O \rightarrow NO_2^- + NO_3^- + 12H^+ + 10e^- \quad (7)$$

$$2NO_3^- + 6H_2O + 10e^- \rightarrow N_2 + 12OH^- \quad (8)$$

$$2NO_2^- + 4H_2O + 6e^- \rightarrow N_2 + 8OH^- \quad (9)$$

2.5 Response surface method experiment (RSM)

2.5.1 Design and result

The RSM was adopted to optimize the 3DES treatment and get a higher simultaneous removal rate of NH_3-N and COD. Experimental design was carried out by custom design

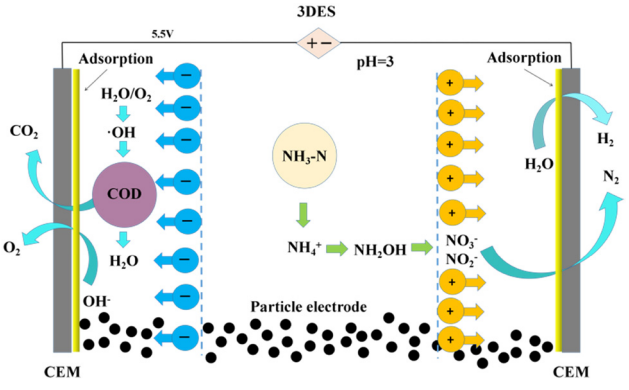

Figure 3: Reaction process diagram of CW treated by 3DES.

Table 3: Factors and levels for the experimental design

Factor	Level		
	1	2	3
A (h)	3.5	4	4.5
B (V)	4.5	5	5.5
C (mm)	13	15	17
D (g)	3.5	4	4.5
E (–)	2	2.5	3

method in JMP software, and the response item were the R_C and R_N. Five parameters, including processing time (*A*), applied voltage (*B*), electrode plate spacing (*C*), mass of CAC (*D*), and initial pH of CW (*E*) were studied and each parameter was set according to single factor experiment results, as shown in Table 2. In addition, design and result are also shown in Table 3, which will be discussed later.

2.5.2 Analysis of the model

The RSM method was employed to analyze the experimental data in Table 4 and the quadratic regression surface model was established after eliminating the non-significant items. The model for R_C and R_N can be calculated by the obtained quadratic regression equations given by Eqs. 10 and 11. Analysis results by stepwise regression method are listed in Tables A1 and A2 (in Appendix), the correlation coefficient (R^2) of the model is 0.9853 and 0.9372, respectively, which indicated that the stepwise regression model was suitable for optimizing the experimental data of the process. Significance tests for the regression model are listed in Tables A3 and A4, respectively. The significant factor for R_C was B and A as well as A*B, C*C, A*D, B*D, and C*D, which means these factors were not a simple linear relationship, in order to get the optimization conditions of the process, interaction effect among these factors was explored by three-dimensional RSM of the quadratic polynomial regression equation, as shown in Figure 4. Sequence for these key factors of R_C was B > A > C > E > D. Meanwhile, the significant factor for R_N was D and A, the sequence was D > A > E > B > C.

$$\begin{aligned} R_C = {} & 70.14 - 0.48x_1 + 1.77x_2 + 0.24x_3 + 0.086x_4 \\ & + 0.13x_5 + 0.04{x_1}^2 + 0.39x_1x_2 + 0.38{x_2}^2 \\ & - 0.23x_1x_3 + 0.02x_2x_3 + 1.10{x_3}^2 + 0.64x_1x_4 \\ & + 0.70x_2x_4 + 0.42x_3x_4 + 0.08{x_4}^2 + 0.24x_1x_5 \\ & - 0.17x_2x_5 + 0.04x_3x_5 - 0.41x_4x_5 - 0.42{x_5}^2 \end{aligned} \quad (10)$$

Table 4: Experimental design and results

No.	Condition	R_C (%)	R_N (%)
1	A3B2C3D1E3	69.9	41
2	A2B3C3D1E3	71.3	40
3	A2B3C2D2E2	72	41.7
4	A1B1C2D1E2	70	38.9
5	A3B2C1D2E2	70.2	42.3
6	A3B3C1D1E3	72.4	41.1
7	A2B3C3D3E1	73.1	43.6
8	A3B1C1D1E1	68	41.2
9	A2B2C2D2E1	69.5	42.3
10	A3B1C3D3E1	68.9	51.4
11	A3B1C1D3E3	68	51.7
12	A1B3C1D3E3	71.8	48.6
13	A3B3C3D1E1	70.8	41.3
14	A2B1C1D1E3	70.4	40.5
15	A2B1C3D2E2	70	41.7
16	A1B3C2D1E1	72.8	39.1
17	A1B2C1D2E2	71	40.1
18	A3B1C1D2E3	68.4	41.3
19	A2B2C2D3E2	70	50.8
20	A2B2C2D1E1	70.3	39.7
21	A2B2C2D3E2	70.6	43.7
22	A1B2C2D2E3	70	40.6
23	A1B1C1D3E1	68.9	42.9
24	A3B3C1D3E1	73.8	51.1
25	A1B3C2D1E2	72.7	39.4
26	A1B1C3D3E3	69.8	49.7
27	A3B3C3D3E3	74.9	51.4

$$\begin{aligned} R_N = {} & 40.85 + 1.58x_1 + 0.18x_2 + 0.02x_3 + 4.16x_4 \\ & + 0.73x_5 - 0.21{x_1}^2 + 0.19x_1x_2 + 0.06{x_2}^2 \\ & - 0.06x_1x_3 - 0.48x_2x_3 + 0.64{x_3}^2 + 1.12x_1x_4 \\ & - 0.005x_2x_4 + 0.15x_3x_4 + 2.73{x_4}^2 - 0.96x_1x_5 \\ & - 0.07x_2x_5 + 0.07x_3x_5 + 0.54x_4x_5 + 0.63{x_5}^2 \end{aligned} \quad (11)$$

where x_1, x_2, x_3, x_4, and x_5 are equal to (processing time-4)/0.5, (applied voltage-5)/0.5, (electrode plate spacing-15)/2, (mass of CAC-4)/0.5, and (effect of the pH-2.5)/0.5, respectively.

A stable maximum point in the test range can be seen on the response surface in Figure 4. Meanwhile, the predictive value of removal rate will be acquired with certain conditions according to Eqs. 10 and 11. R_N and R_C can reach to 52.65% and 74.78% according to the prediction with the conditions of A1B3C3D3E1 and A3B3C1D3E3, respectively, whereas the prediction simultaneous removal rate of NH_3-N and COD would be lower at 51.48% and 74.20% with the conditions of A3B3C3D3E3, which were determined as the optimal process conditions. Thereafter, three parallel experiments were performed in the laboratory with the optimal parameters and the results of R_C were 75.03%,

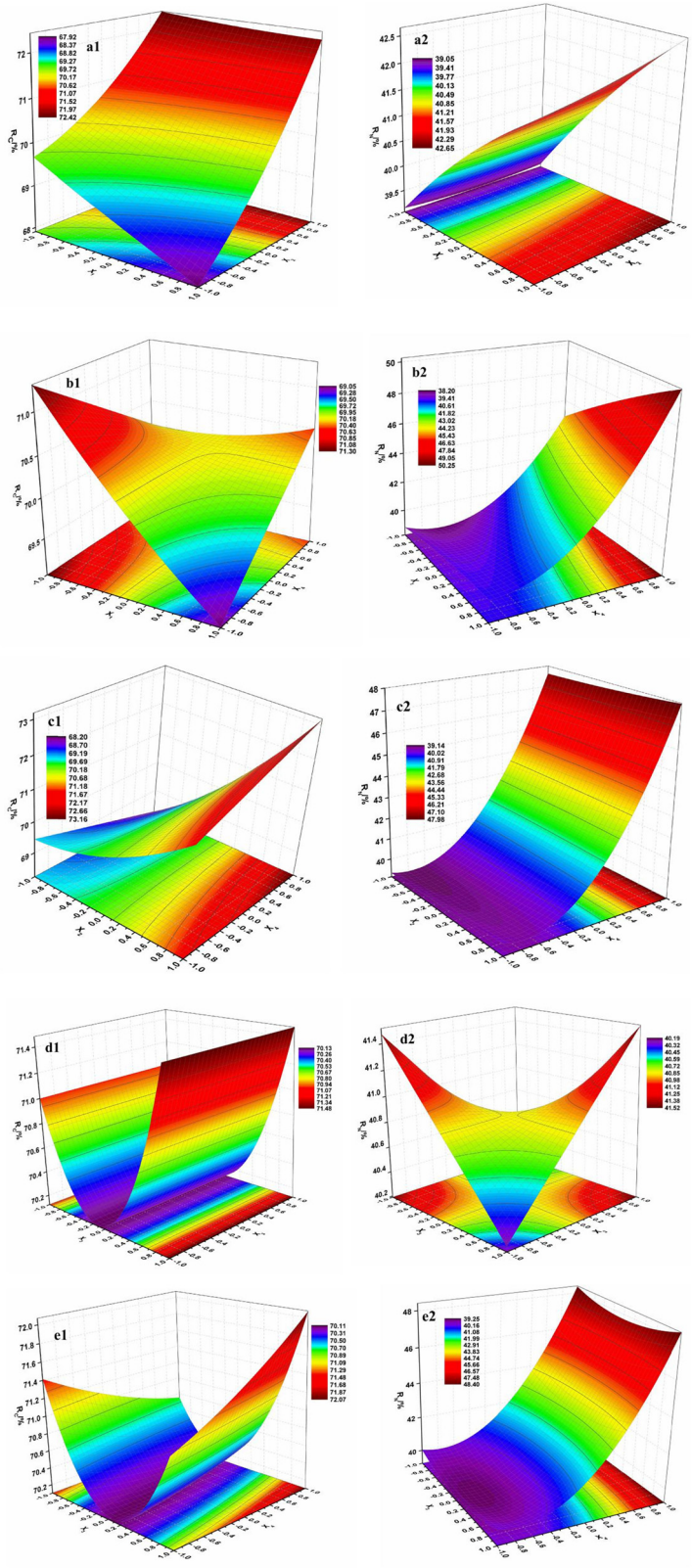

Figure 4: Response surface of factors interaction on R_C and R_N; 1: R_C, 2: R_N, (a) X_1X_2, (b) X_1X_4, (c) X_2X_4, (d) X_3^2, and (e) X_3X_4.

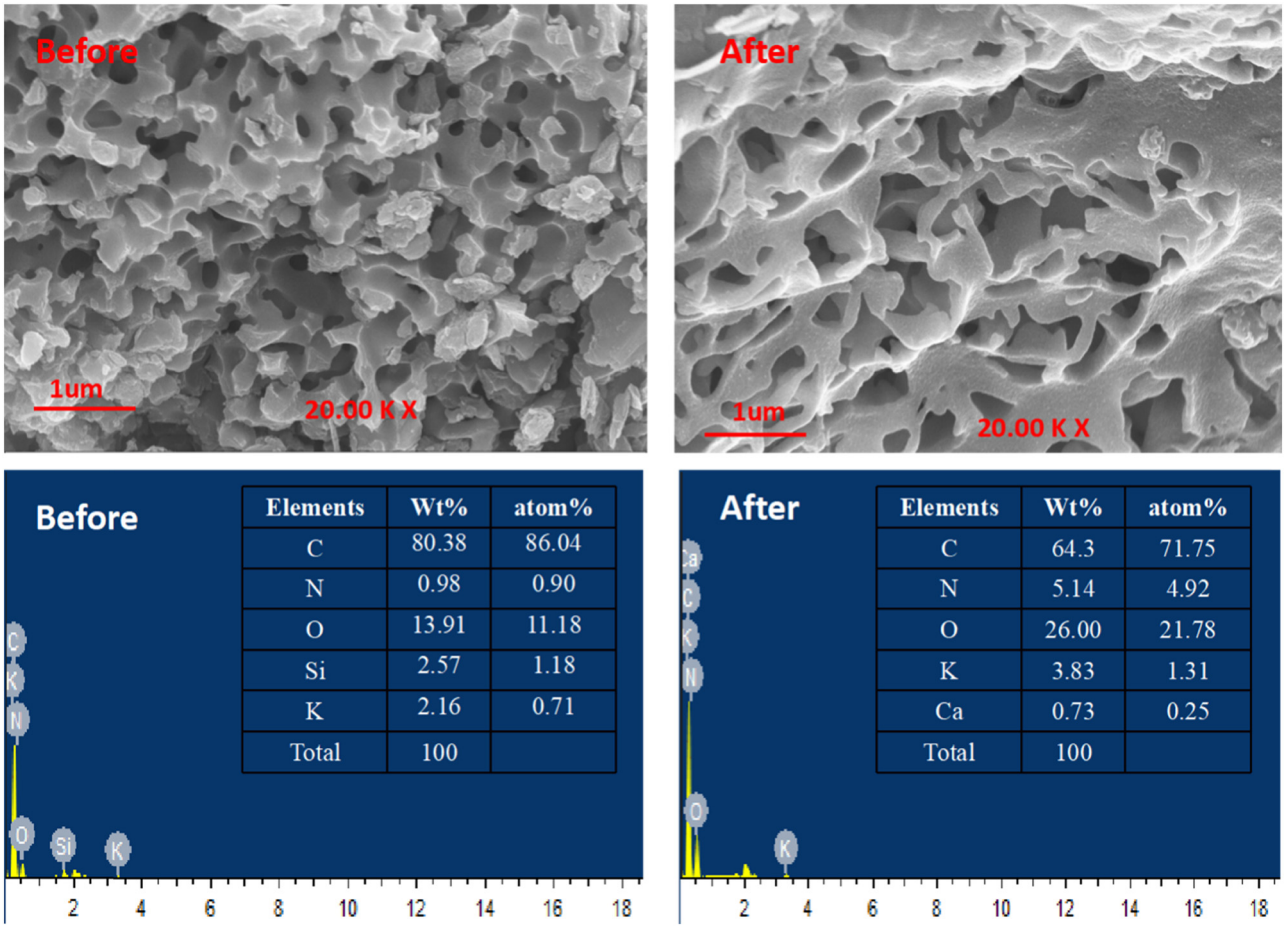

Figure 5: SEM graph and EDS analysis of samples.

74.94%, and 74.07%, respectively, and the results of R_N were 50.71%, 50.94%, and 51.57%, respectively. The experimental data were in good agreement with the predicted data.

2.6 Characterization of CEMs after process

The CEMs after the 3DES treatment were collected for characterization to verify the removal effect of the pollutants.

2.7 SEM-EDS

SEM graphs and EDS analysis of the CEMs are presented in Figure 5. It shows the CEMs structure of multi-pores prepared during the pyrolysis and activation processes. The porous structures were beneficial to the electro-adsorption or electro-chemical reaction and provided ion migration channels leading to higher adsorption capacity or reaction activity. According to the EDS analysis, the atomic percentage of N element in the sample was raised from 0.90% before the treatment to 4.92% after the treatment, indicating the pollutant elements remain in the inner structure of CEMs to achieve the purpose of removing pollutants and reflecting the potential removal performance of the electro-chemical combined oxidation [28].

2.8 FTIR

The FTIR spectra of CEMs before and after the process are shown in Figure 6. Based on Figure 6a, diagnostic band at 3,450 cm^{-1} of both the samples recognized the stretching of hydroxyl group (–OH) which implied that raw materials could promote the reactivity of –OH, facilitating detachment to produce H_2O or conversion to other oxygen-containing functional groups such as C═O and C–O. The peak adsorption at 3,150 cm^{-1} on the sample before the process

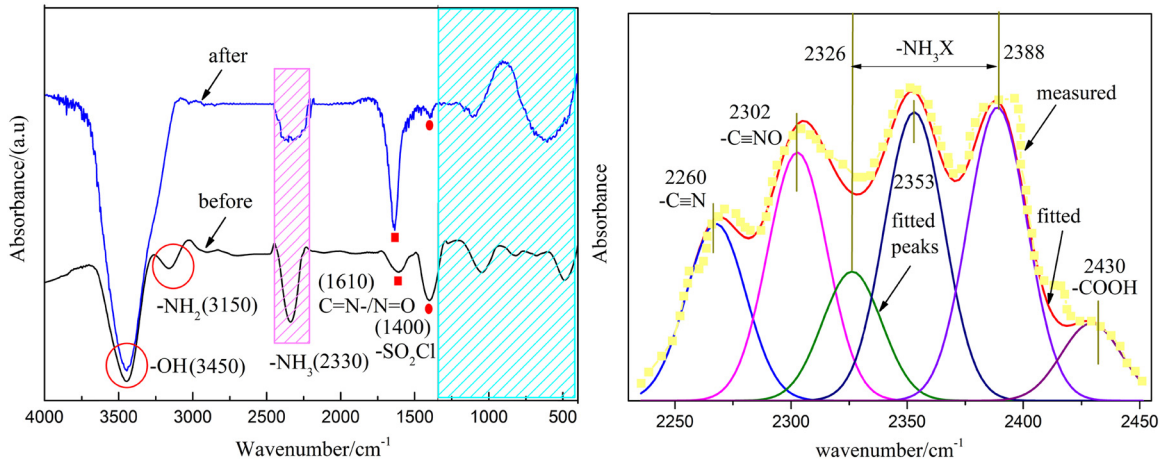

Figure 6: (a) FTIR analysis of CEMs and (b) curve fittings of sample in wavenumber of 2,450–2,230 cm^{-1}.

illustrated the N–H group, which was not observed on the sample after the process, it may be due to the oxygen containing functional groups like –OH groups affected it and shifted its position to lower frequency band intensity and did not show as a peak. The appearance of peak at 2,330 cm^{-1} indicates the presence of $-NH_3$ group, whereas a wide absorption peak (wavenumber from 2,250 to 2,450 cm^{-1}) was formed here on the sample after the process, which may be the result of the superposition of multiple peaks, thus, the curve fitting was carried out in Figure 6b and it will be discussed later. 1,610 cm^{-1} corresponded to C═N– or N═O, it was strengthened after electro-treatment compared to before treatment, indicating the participation of these groups in CW. $-SO_2Cl$ groups on both the samples before and after electro-treatment were recognized at 1,400 cm^{-1} and the only difference between the two curves was the intensity, which may be caused by the interaction effect of the electro-treatment. Six fitted peaks related to –C≡N, –C≡NO, $-NH_3X$ (containing three peaks, and X represents one element of C, N, O, or S), and –COOH are shown in Figure 6b, which reasonably represented the corresponding structures in the matters of CEMs after the process, and certified the removal effect of NH_3-N.

3 Conclusion

It can be concluded that the 3EDS with CEMs is efficient in CW treatment. The method is suitable for simultaneous removal effect of NH_3-N and COD. The optimum conditions for the electrode system of CW treatment using central composite design were found to be at 4.5 h processing time, 5.5 V applied voltage, 17 mm electrode plate spacing, 4.5 g CAC and initial pH of 3 with higher pollutant removal percentage for COD (74.20%) and NH_3-N (51.48%), and the concentrations of 116.1 and 28.7 $mg{\cdot}L^{-1}$, respectively, which nearly conforms to the standard of coke quenching in China (COD 150 $mg{\cdot}L^{-1}$ and NH_3-N 25 $mg{\cdot}L^{-1}$). The RSM greatly optimized the configuration of parameters, and the experimental data was in good agreement with the predicted data, which indicated that the maximum value of simultaneous removal of two pollutants can be reached stably. Applied voltage is the most influential factor in the removal of COD because of the production of hydroxyl radical (˙OH) with extremely strong redox ability by electrolysis of water molecules or oxygen. Whereas the NH_3-N removal mechanism was more likely to be converted to N_2 under low pH conditions. The SEM-EDS and FTIR analysis for existence of N element or N containing groups in CEMs after the process confirmed the removal effect of pollutants. In brief, this 3EDS with CEMs enables the simultaneous removal effect of NH_3-N and COD, which can be used as a simple and cost-effective system for the treatment of CW.

Funding information: The financial support was obtained from the National Natural Science Foundation of China (22065035 and 52062047), Natural Science Foundation of Shaanxi Province of China (2019JLM-44, 2019SF-273, 2018GY-086, and 2020SF-408), Joint foundation of Clean Energy Innovation Institute and Yulin University (Grant. YLU-DNL Fund 2021003), and Science and Technology Foundation of Yulin High-tech Zone (CXY-2020-13).

Author contributions: Ting Su: writing – original draft, writing – review and editing; Wenwen Gao: data curation and software; Xiangdong Xing: formal analysis and investigation; Xinzhe Lan: conceptualization, methodology; Yonghui Song: project administration, visualization.

Conflict of interest: Authors state no conflict of interest.

Data availability statement: All data generated or analyzed during this study are included in this published article and its appendix.

References

[1] National Bureau of Statistics of China, 2020. http://www.stats.gov.cn.

[2] Elawwad A, Naguib A, Abdel-Halim H. Modeling of phenol and cyanide removal in a full-scale coke-oven wastewater treatment plant. Desalin Water Treat. 2020;57:25181–93.

[3] Ren J, Li JF, Li JG, Chen ZL, Cheng FQ. Tracking multiple aromatic compounds in a full-scale coking wastewater reclamation plant: Interaction with biological and advanced treatments. Chemosphere. 2019;222:431–9.

[4] Bu Q, Li Q, Cao Y, Cao. H. A new method for identifying persistent, bioaccumulative, and toxic organic pollutants in coking wastewater. Process Saf Environ Prot. 2020;144:158–65.

[5] Ji Q, Tabassum S, Hena S, Silva CG, Yu G, Zhang Z. A review on the coal gasification wastewater treatment technologies: Past, present and future outlook. Clean Prod. 2016;126:38–55.

[6] Yang Q, Xiong P, Ding P, Chu L, Wang J. Treatment of petrochemical wastewater by microaerobic hydrolysis and anoxic/oxic processes and analysis of bacterial diversity. Bioresour Technol. 2015;196:169–75.

[7] Raper E, Fisher R, Anderson DR, Stephenson T, Soares A. Nitrogen removal from coke making wastewater through a predenitrification activated sludge process. Sci Total Env. 2019;666:31–8.

[8] Zhang M, Yang Q, Zhang J, Wang C, Wang S, Peng Y. Enhancement of denitrifying phosphorus removal and microbial community of long-term operation in an anaerobic anoxic oxic–biological contact oxidation system. Biosci Bioeng. 2016;122:456–66.

[9] Wang J, Ji Y, Zhang F, Wang D, He X, Wang C. Treatment of coking wastewater using oxic-anoxic-oxic process followed by coagulation and ozonation. Carbon Resour Convers. 2019;2:151–6.

[10] Rajeshwar K, Ibanez JG, Swain GM. Electrochemistry and the environment. J Appl Electrochem. 1994;24:1077–91.

[11] Feng L, Li XY, Gan LH, Xu J. Synergistic effects of electricity and biofilm on rhodamine B (RhB) degradation in three-dimensional biofilm electrode reactors (3D-BERs). Electrochim Acta. 2018;290:165–75.

[12] Ji J, Liu Y, Yang XY, Xu J, Li XY. Multiple response optimization for high efficiency energy saving treatment of rhodamine B wastewater in a three-dimensional electrochemical reactor. J Env Manag. 2018;218:300–8.

[13] Shen B, Wen XH, Huang X. Enhanced removal performance of estriol by a three-dimensional electrode reactor. Chem Eng J. 2017;327:597–607.

[14] Zhang C, Jiang Y, Li Y, Hu Z, Zhou L, Zhou M. Three-dimensional electrochemical process for wastewater treatment: A general review. Chem Eng J. 2013;228:455–67.

[15] Ting S, Yonghui S, Xinzhe L, Wenwen G. Adsorption optimized of the coal-based material and application for cyanide wastewater treatment. Green Proc Synth. 2019;8:391–8.

[16] Chen Y, Song Y, Chen Y, Zhang X, Lan X. Comparative experimental study on the harmless treatment of cyanide tailings through slurry electrolysis. Sep Purif Technol. 2020;251:117314.

[17] Tyagi M, Kumari N, Jagadevan S. A holistic Fenton oxidation-biodegradation system for treatment of phenol from coke oven wastewater: Optimization, toxicity analysis and phylogenetic analysis. J. Water Process Eng. 2020;37:101475.

[18] Wu Z, Zhu W, Liu Y, Peng P, Li X, Zhou X, et al. An integrated three-dimensional electrochemical system for efficient treatment of coking wastewater rich in ammonia nitrogen. Chemosphere. 2020;246:125703.

[19] Pitás V, Somogyi V, Kárpáti Á, Thury P, Fráter T. Reduction of chemical oxygen demand in a conventional activated sludge system treating coke oven wastewater. J Clean Prod. 2020;273:122482.

[20] Wang M, He L, Wang M, Chen L, Yao S, Jiang W, et al. Simultaneous removal of NH_3-N and COD from shale gas distillate via an integration of adsorption and photo-catalysis: A hybrid approach. J Environ Manag. 2019;249:109342.

[21] Barros WRP, Ereno T, Tavares AC, Lanza MRV. In situ electrochemical generation of hydrogen peroxide in alkaline aqueous solution by using an unmodified gas diffusion electrode. ChemElectroChem. 2015;2(5):714–9.

[22] Reis RM, Beati AAGF, Rocha RS, Assumpção MHMT, Santos MC, Bertazzoli R, et al. Use of gas diffusion electrode for the in situ generation of hydrogen peroxide in an electrochemical flow-by reactor. Ind Eng Chem Res. 2012;51(2):649–54.

[23] Bolger PT, Szlag DC. An electrochemical system for removing and recovering elemental mercury from a gas stream. Env Sci Technol. 2002;36(20):4430–5.

[24] Wang SY, Yang XY, Meng HS, Zhang YC, Li XY, Xu J. Enhanced denitrification by nano α-Fe_2O_3 induced self-assembled hybrid biofilm on particle electrodes of three-dimensional biofilm electrode reactors. Env Int. 2019;125:142–51.

[25] Brillas E, Sires I, Oturan MA. Electro-Fenton process and related electrochemical technologies based on Fenton's reaction chemistry. Chem Rev 2009;109:6570–631.

[26] Yang G, Li Y, Yang S, Liao J, Cai X, Gao Q, et al. Surface oxidized nano-cobalt wrapped by nitrogen-doped carbon nanotubes for efficient purification of organic wastewater. Sep Purif Technol. 2021;259:118098.

[27] Rena G, Zhoua M, Zhang Q, Xua X, Lia Y, Su P. A novel stacked flow-through electro-Fenton reactor as decentralized system for the simultaneous removal of pollutants (COD, NH_3-N and TP) and disinfection from domestic sewage containing chloride ions. Chem Eng J. 2020;387:124037.

[28] Cao L, Yang J, Xu Y, Sun W, Shen Q, Zhou J, et al. The coupling use of electro-chemical and advanced oxidation to enhance the gaseous elemental mercury removal in flue gas. Sep Purif Technol. 2021;257:117883.

Appendix

$$R_C = \frac{C_0 - C_1}{C_0} \times 100\% \quad \text{(A1)}$$

$$R_N = \frac{C_0' - C_1'}{C_0'} \times 100\% \quad \text{(A2)}$$

where C_0 is the initial concentration of COD, mg·L^{-1} and C_1 is the concentration of COD after treatment, mg·L^{-1}. C_0' is the initial concentration of NH_3-N, mg·L^{-1} and C_1' is the concentration of NH_3-N after treatment, mg·L^{-1}.

Table A1: Analysis of variance for the regression model (R^2 = 0.9853)

Source	D_f	Sum of square	Mean square	F value	P value
Model	20	92.1433	4.6072	20.1338	0.0006
Error	6	1.3729	0.2283		
Total	26	93.5163			

Table A2: Analysis of variance for the regression model (R^2 = 0.9372)

Source	D_f	Sum of square	Mean square	F value	P value
Model	20	507.0214	25.3511	4.4729	0.0356
Error	6	34.0061	5.6677		
Total	26	541.0274			

Table A3: Significance test for the regression coefficients

Source	D_f	Sum of square	F value	P value
A	1	3.3815	14.7760	0.0085*
B	1	53.7118	234.7263	0.0001*
C	1	0.8807	3.8490	0.0974
D	1	0.1369	0.5987	0.4685
E	1	0.2913	1.2732	0.3023
A*A	1	0.0067	0.0295	0.8693
A*B	1	1.8251	7.9759	0.0302*
B*B	1	0.5784	2.5279	0.1630
A*C	1	0.5771	2.5219	0.1634
B*C	1	0.0047	0.0206	0.8907
C*C	1	4.2796	18.7022	0.0050*
A*D	1	4.4455	19.4272	0.0045*
B*D	1	6.6128	28.8987	0.0017*
C*D	1	2.2320	9.7540	0.0205*
D*D	1	0.2222	0.0971	0.7658
A*E	1	0.6226	2.7207	0.1501
B*E	1	0.3247	1.4189	0.2786
C*E	1	0.0212	0.0926	0.7712
D*E	1	2.3744	10.3764	0.0181*
E*E	1	0.6217	2.7170	0.1504

"*" means significant influence factor.

Table A4: Significance test for the regression coefficients

Source	D_f	Sum of square	F value	P value
A	1	36.2393	6.3940	0.0448*
B	1	0.5736	0.1012	0.7612
C	1	0.0035	0.0006	0.9809
D	1	320.2786	56.5097	0.0003*
E	1	9.1064	1.6067	0.2519
A*A	1	0.1794	0.0317	0.8646
A*B	1	0.4500	0.0794	0.7876
B*B	1	0.0136	0.0024	0.9625
A*C	1	0.0357	0.0063	0.9393
B*C	1	2.5664	0.4528	0.5621
C*C	1	1.4702	0.2594	0.6287
A*D	1	13.7521	2.4264	0.1703
B*D	1	0.0003	0.0001	0.9945
C*D	1	0.2729	0.0482	0.8336
D*D	1	27.2507	4.8081	0.0708
A*E	1	10.1499	1.7908	0.2293
B*E	1	0.0608	0.0107	0.9209
C*E	1	0.0608	0.0107	0.9209
D*E	1	4.1301	0.7287	0.4621
E*E	1	1.3543	0.2389	0.6423

"*" means significant influence factor.